Supplementary information for

Combination of Adenosine Blockade and Ferroptosis for Photo-Immunotherapy of Triple Negative Breast Cancer with Aptamer Modified Copper Sulfide

Xingyu Zhang†, Chengyu Shi†, Qiao Liu, Yuting Zhong, Lipeng Zhu, Yuetao Zhao*

X. Zhang, C. Shi, Q. Liu, Y. Zhong, Dr. L, Zhu, Prof. Y. Zhao

Department of Biochemistry and Molecular Biology, School of Life Sciences, Central South University, Changsha, 410012, China.

†Xingyu Zhang and Chengyu Shi contributed equally to this work.

*Correspondence:

Yuetao Zhao, E-mail: ytzhao@csu.edu.cn

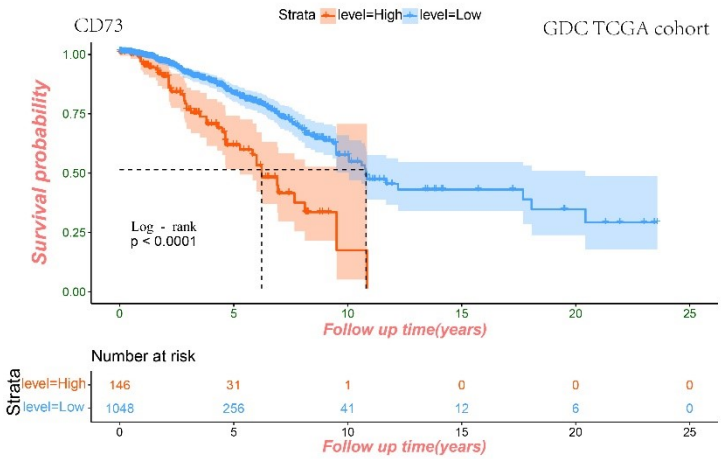

Figure S1. Higher expression of CD73 was associated with poor prognosis in breast cancer. P < 0.05 is considered as significant.

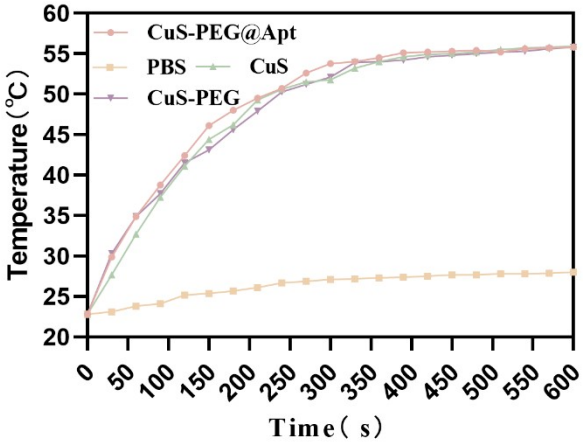

Figure S2. Temperature variation of different nanomaterials and PBS upon 808 nm laser irradiation (1.5 W cm^{-2}, 10 min).

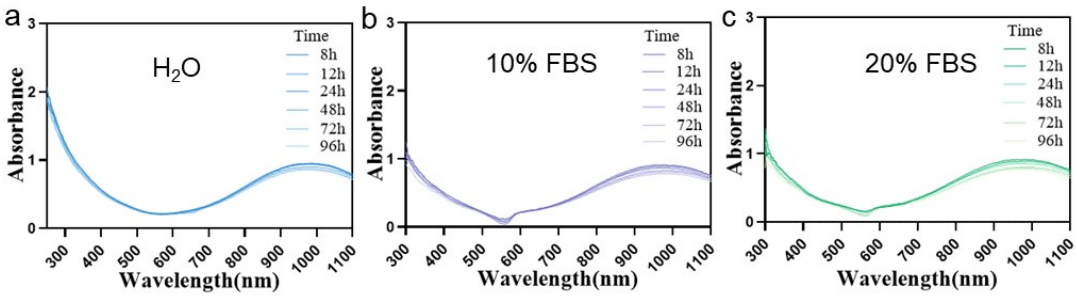

Figure S3. Absorption of CuS-PEG@Apt incubated in **a**) water, **b**) 10% FBS, and **c**) 20% FBS at different times.

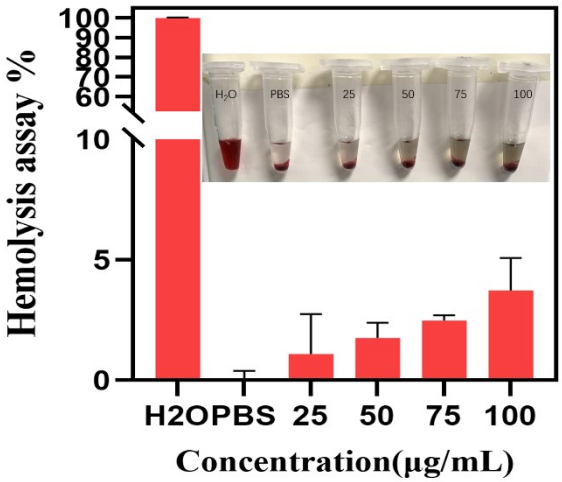

Figure S4. Hemolysis ratio and photos of red blood cells cultured with CuS-PEG@Apt of different concentrations.

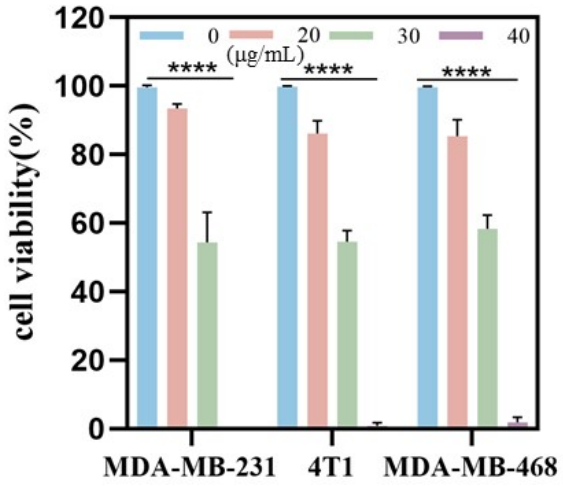

Figure S5. Corresponding quantitative analysis of calcein-AM/propidium iodide (PI) double staining of the MDA-MB-231, 4T1, and MDA-MB-468 cells after different treatments.

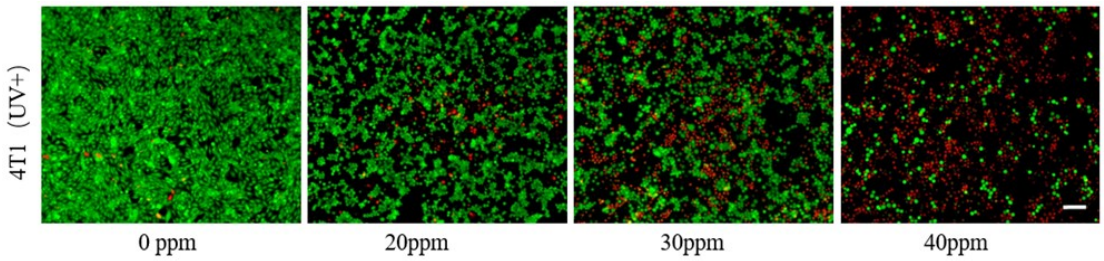

Figure S6. Calcein-AM/ PI staining of the 4T1 cells after treatment of CuS-PEG@Apt (0, 20, 30 and 40 ppm) plus UV irradiation (410 nm, 120 mW cm^{-2}, 30 min). Scale bar: 50 μm.

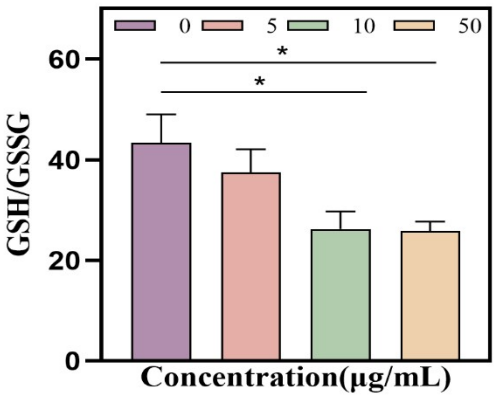

Figure S7. GSH/GSSG ratio of MD A-MB-231 cells detected by GSH and GSSG Assay Kit.

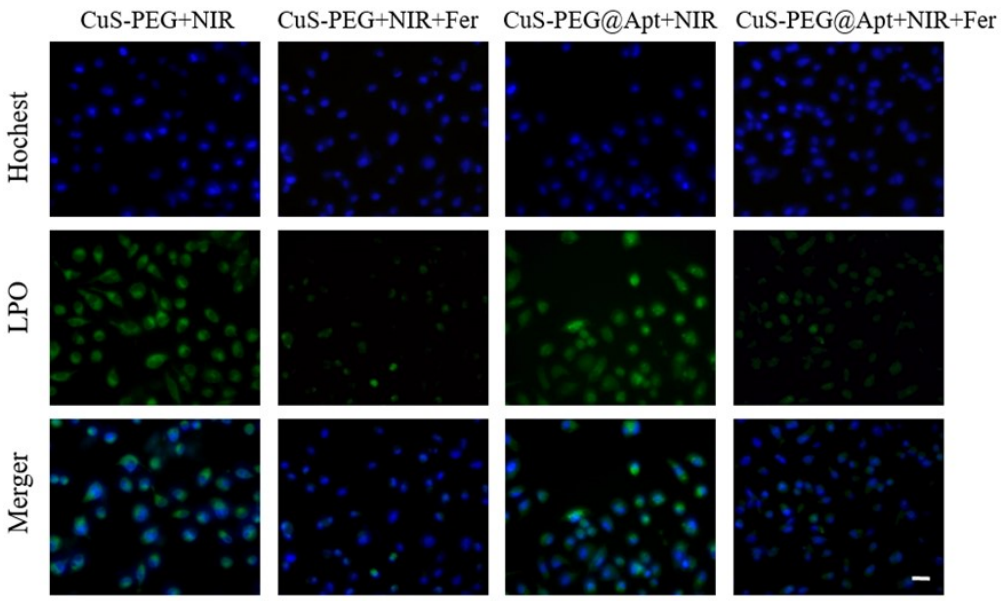

Figure S8. Immunofluorescence microscope images of lipid peroxidation (LPO) in MDA-MB-231 cells with or without ferrostatin-1(Fer) treated with nanoparticle plus irradiation. Scale bar: 20 μm.

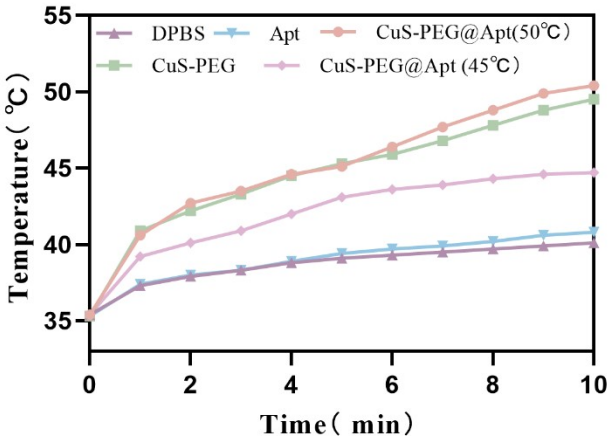

Figure S9. Temperature changes of tumor sites of 4T1 bearing mice upon 808 nm laser irradiation.

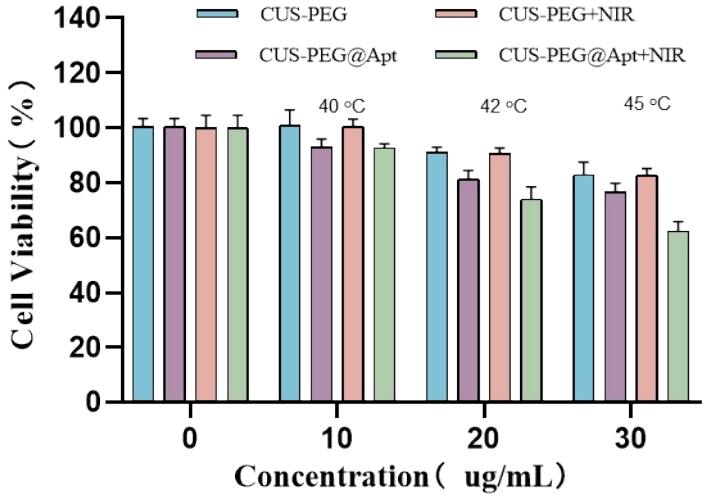

Figure S10. Cell viability of HACAT cells treated with different concentrations of CuS-PEG@Apt and irradiated at different temperature.

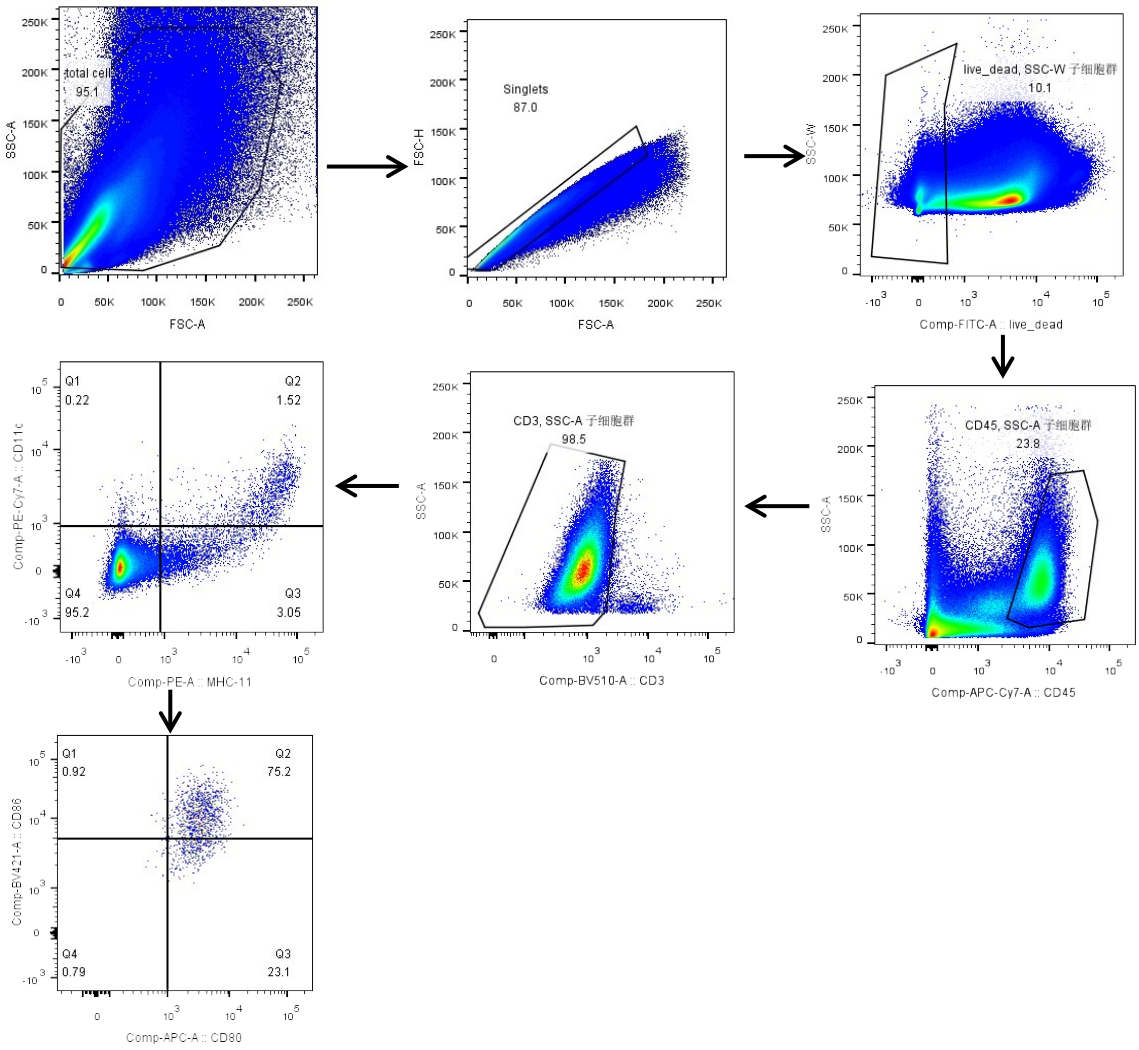

Figure S11. The gating strategy for the flow cytometric analysis of $CD80^{+}CD86^{+}$ DCs in Figure 6d.

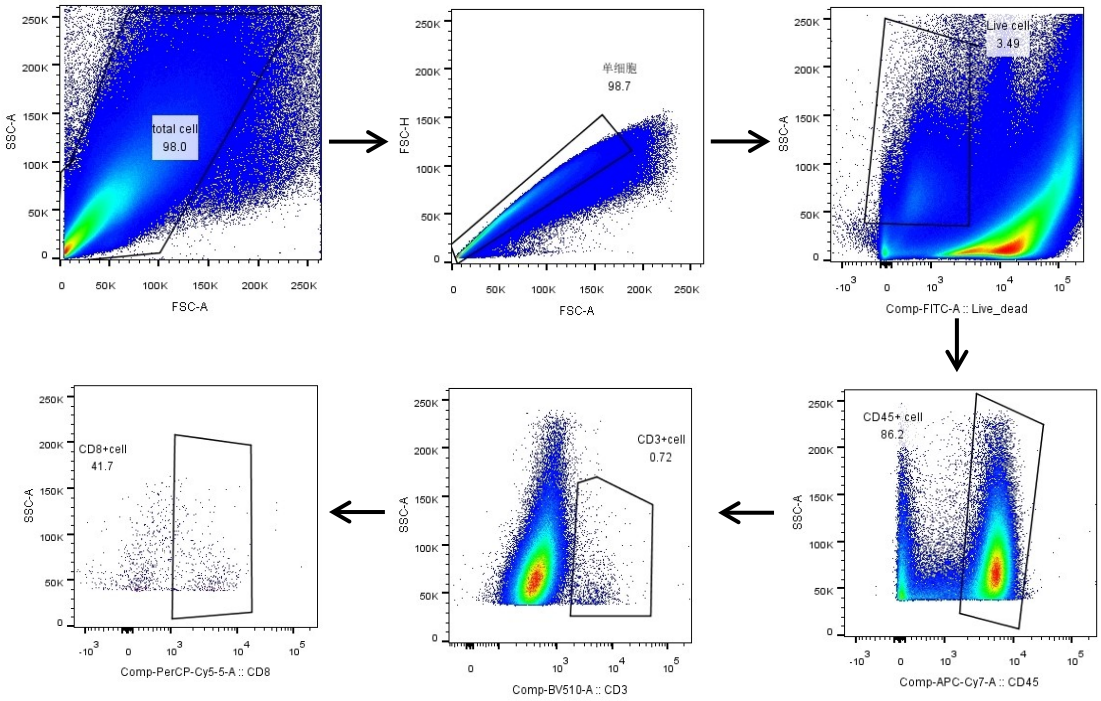

Figure S12. The gating strategy for the flow cytometric analysis of $CD8^+$ T cells in Figure 6e.

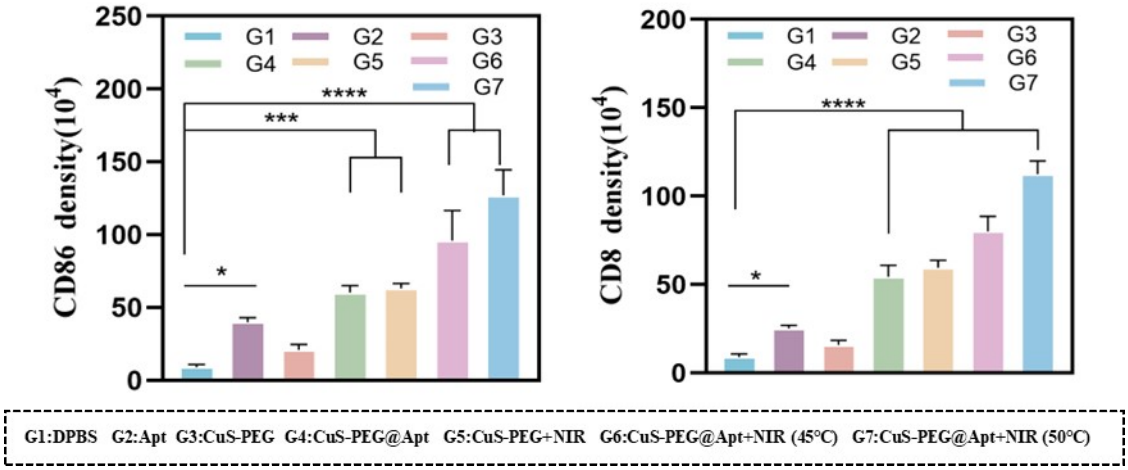

Figure S13. Corresponding quantitative analysis of the fluorescence intensity of **a**) CD86, and **b**) CD8 in the tumor slides of 4T1 bearing mice with treated with different treatments.

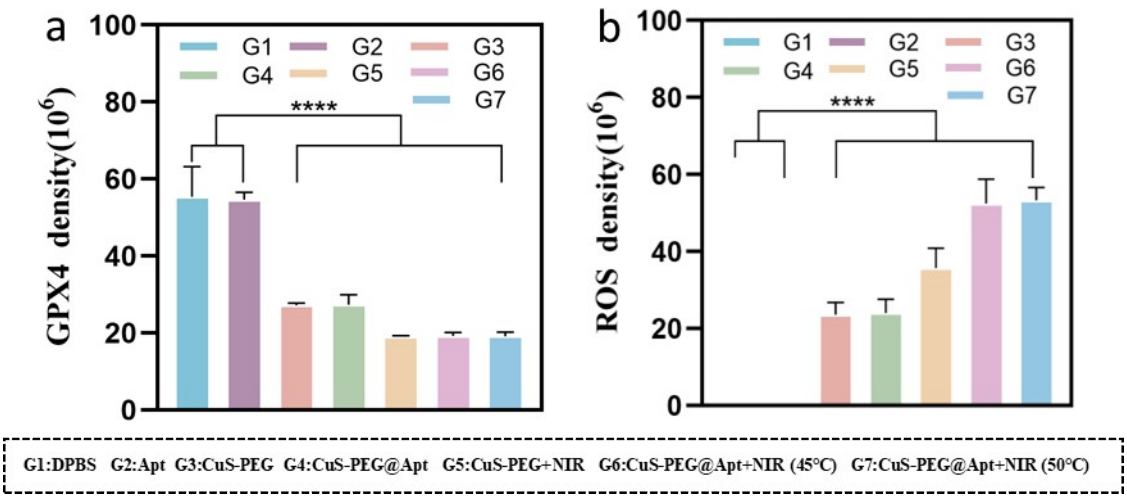

Figure S14. Corresponding quantitative analysis of the fluorescence intensity of **a**) GPX4, and **b**) ROS in the tumor slides of 4T1 bearing mice with treated with different treatments.